Renewable and Sustainable Energy Reviews 14 (2010) 374–383

Contents lists available at ScienceDirect

Renewable and Sustainable Energy Reviews

journal homepage: www.elsevier.com/locate/rser

Study of cavitation in hydro turbines—A review

Pardeep Kumar, R.P. Saini *

Alternate Hydro Energy Centre, Indian Institute of Technology, Roorkee 247667, India

ARTICLE INFO

Article history:
Received 29 April 2009
Accepted 13 July 2009

Keywords:
Hydro turbine
Cavitation
Rotating machinery
Computational fluid dynamics

ABSTRACT

Reaction turbines basically Francis turbines and propeller/Kaplan turbines are suitable for medium and low head hydropower sites. The management of the small hydropower plants is an important factor, for achieving higher efficiency of hydro turbines with time. Turbines show declined performance after few years of operation, as they get severely damaged due to various reasons. One of the important reasons is erosive wear of the turbines due to cavitation. Reaction turbines, however are more prone to cavitation especially Francis turbines where a zone in the operating range is seriously affected by cavitation and considered as forbidden zone. Cavitation is a phenomenon which manifests itself in the pitting of the metallic surfaces of turbine parts because of the formation of cavities. In the present paper, studies undertaken in this field by several investigators have been discussed extensively. Based on literature survey various aspects related to cavitation in hydro turbines, different causes for the declined performance and efficiency of the hydro turbines and suitable remedial measures suggested by various investigators have been discussed.

© 2009 Elsevier Ltd. All rights reserved.

Contents

1. Introduction

Energy is the basic requirement for economic development. Every sector of a country's economy (industry, agricultural, transport, commercial and domestic) needs input of energy. The installed electricity generating capacity in India at present is nearly 128 GW which is generated 66% through thermal, 26% through hydro, 3% through nuclear and 5% through other renewables. According to International Energy Agency (IEA), a threefold rise in India's generation capacity is expected by 2020 [1]. As the non-renewable fossil energy sources continues to deplete, and realizing the summits held at Brazil and Kyoto, to reduce the greenhouse gas emissions, hydropower has moved towards the top power development option to meet the increasing energy demand. Small hydropower (SHP) has grown substantially in the last 10 years. Among all the renewable energy sources available, small hydropower is considered as the most promising source of energy. The hydraulic turbine being the heart of a SHP plant transforms the potential energy of water into mechanical energy in the form of rotation of shaft. Hydraulic turbines can be broadly classified into two categories according to action of water on moving blades. Hydro turbines classification based on action of water over runner are impulse turbines and reaction turbines. Impulse turbines are high head turbines and operate at atmospheric pressure. At some of hydropower sites where head is relatively low and discharge is of medium or high order it becomes difficult to operate an impulse type turbine as sufficient speed may not be obtained to drive the end use machine at such sites. It is therefore reaction turbines are suggested to be used and these considered high speed turbines under medium and low head. These turbines are closed turbines

* Corresponding author. Tel.: +91 1332 285841; fax: +91 1332 273517/60.
E-mail address: rajsafah@iitr.ernet.in (R.P. Saini).

1364-0321/$ – see front matter © 2009 Elsevier Ltd. All rights reserved.
doi:10.1016/j.rser.2009.07.024

operate under variable pressure. Further these turbines are more prone to cavitation and a zone in the operating range is seriously affected by cavitation and considered as forbidden zone especially in case of Francis turbine. The management of the small hydropower plants for achieving higher efficiency of hydro turbines with time is an important factor, but the turbines show declined performance after few years of operation as they get severely damaged due to various reasons. One of the important reasons is erosive wear of the turbines due to high content of abrasive material during monsoon and cavitation [2]. According to the Bernoulli's equation, if the velocity of flow increases, the pressure will fall. In case of liquid, the pressure cannot fall below vapor pressure, the vapor pressure is defined as the pressure at which liquid is vaporized at a given temperature, which depends upon the temperature and height above mean sea level of the site. Whenever the pressure in any turbine part drops below the evaporation pressure, the liquid boils and large number of small bubbles of vapors are formed. It may happen that a stream of water cuts short of its path giving rise to eddies and vortices which may contain voids or bubbles. These bubbles mainly formed on account of low pressure, are carried by the stream to higher pressure zones where the vapors condense and the bubbles suddenly collapse, as the vapors are condensed to liquid again. This results in the formation of a cavity and the surrounding liquid rushes to fill it. The streams of liquid coming from all directions collide at the center of cavity giving rise to a very high local pressure whose magnitude may be as high as 7000 atm. Formation of cavity and high pressure are repeated many thousand times a second. This causes pitting on the metallic surface of runner blades or draft tube. The material then fails by fatigue, added perhaps by corrosion. Some parts of turbine such as runner blades may be torn away completely by this process. The phenomenon which manifests itself in the pitting of the metallic surfaces of turbine parts is known as cavitation because of the formation of cavities. Due to sudden collapsing of the bubbles on the metallic surface, high pressure is produced and metallic surfaces are subjected to high local stresses. Thus the surfaces are damaged [3]. Prof. D. Thoma suggested a dimensionless number, called as Thoma's cavitation factor σ (sigma), which can be used for determining the region where cavitation take place in reaction turbines:

$$\sigma = \frac{H_b - H_s}{H} \tag{1}$$

where H_b is the barometric pressure head in m of water, H_s is the suction pressure at the outlet of reaction turbine in m of water or height of the turbine runner above the tail water surface, H is the net head on the turbine in m of water [4].

The value of Thoma's cavitation factor (σ) for a particular type of turbine is calculated from the Eq. (1). This value of Thoma's cavitation factor (σ) is compared with critical cavitation factor (σ_c) for that type of turbine. If the value of σ is greater than σ_c cavitation will not occur in that turbine.

For safe operation (cavitation-free) of turbine, it is evident that:

$$\sigma > T_c \tag{2}$$

The following empirical relationships are used for obtaining the value of T_c for different turbines [5].

For Francis turbines,

$$T_c = 431 \times 10^{-8} \times N_s^2 \tag{3}$$

For propeller turbines,

$$T_c = 0.28 + \left[\frac{1}{7.5 \times (N_s/380.78)^3}\right] \tag{4}$$

where N_s is the specific speed of turbine.

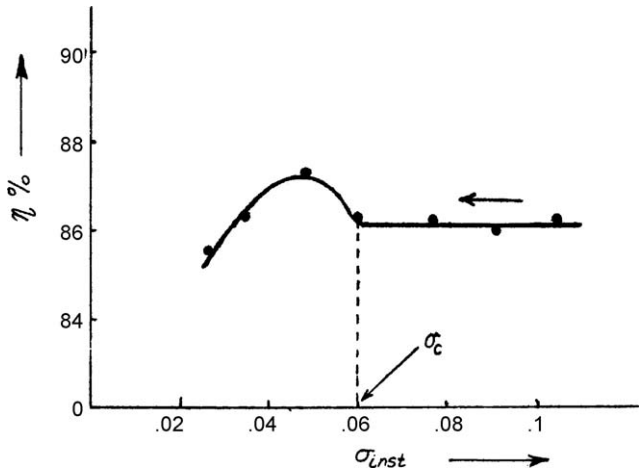

Fig. 1. Variation of efficiency with respect to cavitation factor, σ.

Fig. 1 shows the variation of Thoma's cavitation factor (σ) with efficiency. With increase in suction head (H_s), a corresponding decrease in σ is obtained and this has no effect on the turbine performance as is seen from constant efficiency trend. A stage is however reached when any further increase in suction head (H_s) deteriorates the turbine performance and the turbine efficiency falls. The critical value of cavitation coefficient, T_c is determined by this point marking the change in the trend of efficiency [5].

The present paper discusses the studies carried out by various investigators in order to determine the effect of cavitation and identify the gaps for future studies.

2. Theoretical investigations

Kjolle [6] studied the causes of damages in hydro turbines and found that the main causes of damage of water turbines were due to cavitation problems, sand erosion, material defects and fatigue. The turbine parts exposed to cavitation are the runners and draft tube cones for the Francis and Kaplan turbines. The effect of cavitation erosion was found to be reduced by improving the hydraulic design and production of components, adopting erosion resistant materials and arrangement of the turbines for operations within the good range of acceptable cavitation conditions.

Duncan [7] provided information about cavitation, cavitation repair, cavitation damage inspection, date of inspection, cause of pitting, runner modifications, cavitation pitting locations, methods of cavitation pitting repair, and areas of high stress in runner. Typical areas of cavitation pitting were found as shown in Fig. 2.

Farhat et al. [8] illustrated the benefits of the cavitation monitoring in hydraulic turbines using a vibratory approach. This technique was used in a large Francis turbine in order to validate as light modification of its distributor, which was intended to reduce the cavitation aggressiveness and thereby the related erosion. Cavitation-induced vibrations were measured in fixed parts of the turbine prototype and compared to those measured in a similar and non-rehabilitated turbine.

Karimi and Avellan [9] presented a new cavitation erosion device producing vortex cavitation. A comparative study between various cavitation erosion situations was carried out to verify the ability of this vortex cavitation generator to produce realistic cavitation erosion with respect to that observed in hydraulic machinery. Hardened superficial layers in specimens exposed to flow cavitation were found a thicker than those in vibratory cavitation, which leads to higher erosion rates.

Huixuan et al. [10] carried out an on-line monitoring system for water turbines. Both audible sound (20 Hz–20 kHz) and

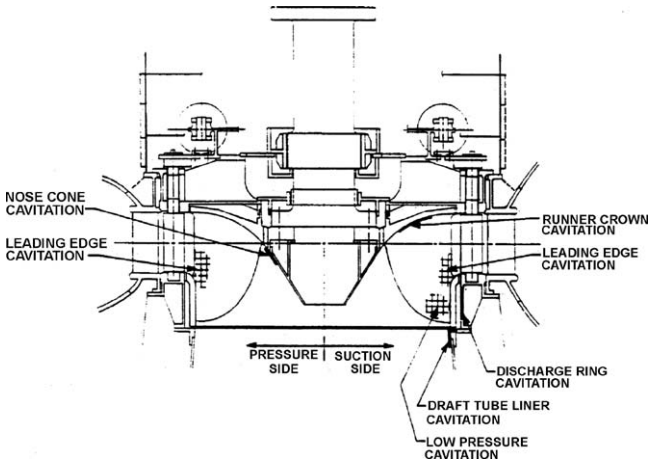

Fig. 2. Francis turbine—typical areas of cavitation pitting.

ultrasound (50–300 kHz) were continuously monitored. The signal characteristics such as standard deviation, noise level and frequency compositions were evaluated. The evaluation results were stored in database in association with the operating condition donated by water head and wicket gate opening (or power output). According to the frequency characteristics, the sound emitted by cavitation was distinguished from the others such as water flow sound and mechanical sound. The cavitation intensity on different water head and power were traced out. The degree of cavitation erosion was estimated according to the cavitation intensity at a fixed operating condition such as rated power and designed water head.

Alligné et al. [11] studied the hydroelectric power plants for their ability to cover variations of the consumption in electrical power networks. In order to follow this changing demand, hydraulic machines were subjected to off-design operation. In that case, the swirling flow leaving the runner of a Francis turbine may act under given conditions as an excitation source for the whole hydraulic system. In high load operating conditions, vortex rope behaved as an internal energy source which leads to the self-excitation of the system. The aim of this paper was to identify the influence of the full load excitation source location with respect to the eigen modes shapes on the system stability.

3. Experimental studies

Escalera et al. [12] carried out an experimental investigation in order to evaluate the detection of cavitation in actual hydraulic turbines. The methodology was based on the analysis of structural vibrations, acoustic emissions and hydrodynamic pressures measured in the machine. The results obtained for the various types of cavitation found in the selected machines were presented and discussed in detail. Various types of cavitation in Francis turbines were found are as shown in Fig. 3. In traveling bubble, the generalized Rayleigh–Plesset equation was found valid approximation of the bubble growth and it can be solved to find the radius of the bubble, $R_B(t)$; provided that the bubble pressure, $P_B(t)$; and the infinite domain pressure, $P_\infty(t)$; are known. The equation is expressed as:

$$\frac{P_B(t)-P_\infty(t)}{\rho}=R_B\frac{d^2R_B}{dt^2}+\frac{3}{2}\left(\frac{dR_B}{dt}\right)^2+\frac{4\nu}{R_B}\frac{dR_B}{dt}+\frac{2\gamma}{\rho R_B} \tag{5}$$

where ν is the kinematic viscosity, 'γ' is the surface tension and 'ρ' is the density.

Bajic [13] carried out noise sampling, signal processing and analysis and data processing, analysis and interpretation in vibro-acoustic diagnostics of turbine cavitation. These were investigated in a series of prototype and model experiments by several weak points of the practice and were identified as shown in Fig. 4. Improvements and new techniques were developed. These techniques enabled extraction of data on cavitation details and early detection of detrimental effects met in turbine exploitation. A brief review of weak points of the practice, developed improvements, and new techniques, as well as examples of application was presented. Noise power, $I(P)$, at the turbine power P, used as an estimate of the cavitation intensity, could be simply modeled by the exponential rule:

$$I(P)=\sum_{m=1}^{M}I_m \tag{6}$$

where I_m is its relative amplitude in the fully developed stage.

Zuo and co-workers [14] carried out a study related to cavitation associated pressure fluctuations in hydraulic systems which was an important phenomenon that affected the design, operation and safety of systems such as hydropower plant, pumping station, rocket engine fuel system, water distribution network, etc. (Fig. 5). The physical model of cavitation cloud in the system was assumed as an exciter, which had its own characteristic frequency (f_{cav}) rather than simply a lumped capacitance (C) and, f_{cav} was a function of cavitation number, and operating condition (Q_1, n_1). In turbo-machinery system, frequency was expressed as:

$$f_{cav}=f_{cav}(\sigma,n_1,Q_1) \tag{7}$$

Wen-quan et al. [15] carried out investigations on turbulent flow in a 3D blade passage of a Francis hydro turbine and flow was simulated with the Large Eddy Simulation (LES) to investigate the spatial and temporal distributions of the turbulence. The computed pressures on the pressure and suction sides agreed with the measured data for a working test turbine model. In LES, large-scale structures could be obtained from the solution of the filtered Navier–Stokes equations, in which the structures smaller than the grid size need to be modeled is expressed as:

$$\frac{\partial\overline{u}_i}{\partial t}+\frac{\partial}{\partial x_j}(\overline{u}_i\overline{u}_j)=-\frac{\partial\overline{P}}{\partial x_i}+\frac{\partial}{\partial x_j}\left[\upsilon\left(\frac{\partial\overline{u}_i}{x_j}+\frac{\partial\overline{u}_j}{\partial x_i}\right)\right]-\frac{\partial\tau_{ij}}{\partial x_j}-2\omega\varepsilon_{i3k}\overline{u}_k \tag{8}$$

where $\bar{P}=\bar{p}-\omega^2r^2/2$, $\bar{u}_i$ is the large-scale relative velocity, $\overline{p}_i$ is the pressure divided by the fluid mass density, ω is the constant angular velocity around the $x3$-axis, r is the radial distance to the $x3$-axis, ε_{i3k} is a circular replacement tensor, ν is the kinetic viscosity, and $\tau_{ij}=u_iu_j-\overline{u}_i\overline{u}_j$ is the SGS stresses.

Escaler et al. [16] carried out work to improve the cavitation erosion prediction methodology in hydro turbines by the use of onboard vibration measurements taken on the rotating shaft. It was discussed whether the use of the vibration from the shaft as an alternative to the bearing ones should be an advantage to infer the absolute erosive forces taking place on the runner blades.

Athavale et al. [17] investigated a new "full cavitation model" developed for performance predictions of engineering equipment under cavitating conditions. All the test cases with cavitation showed plausible results (no negative pressures, and good convergence characteristics). Computations on the water jet pump for non-condensable gas concentrations showed sizeable changes in the pump head developed. The vapor transport equation governing the vapor mass fraction, f, is given as:

$$\frac{\partial}{\partial t}(\rho f)+\nabla(\rho V f)=\nabla(\Gamma\nabla f)+R_e-R_c \tag{9}$$

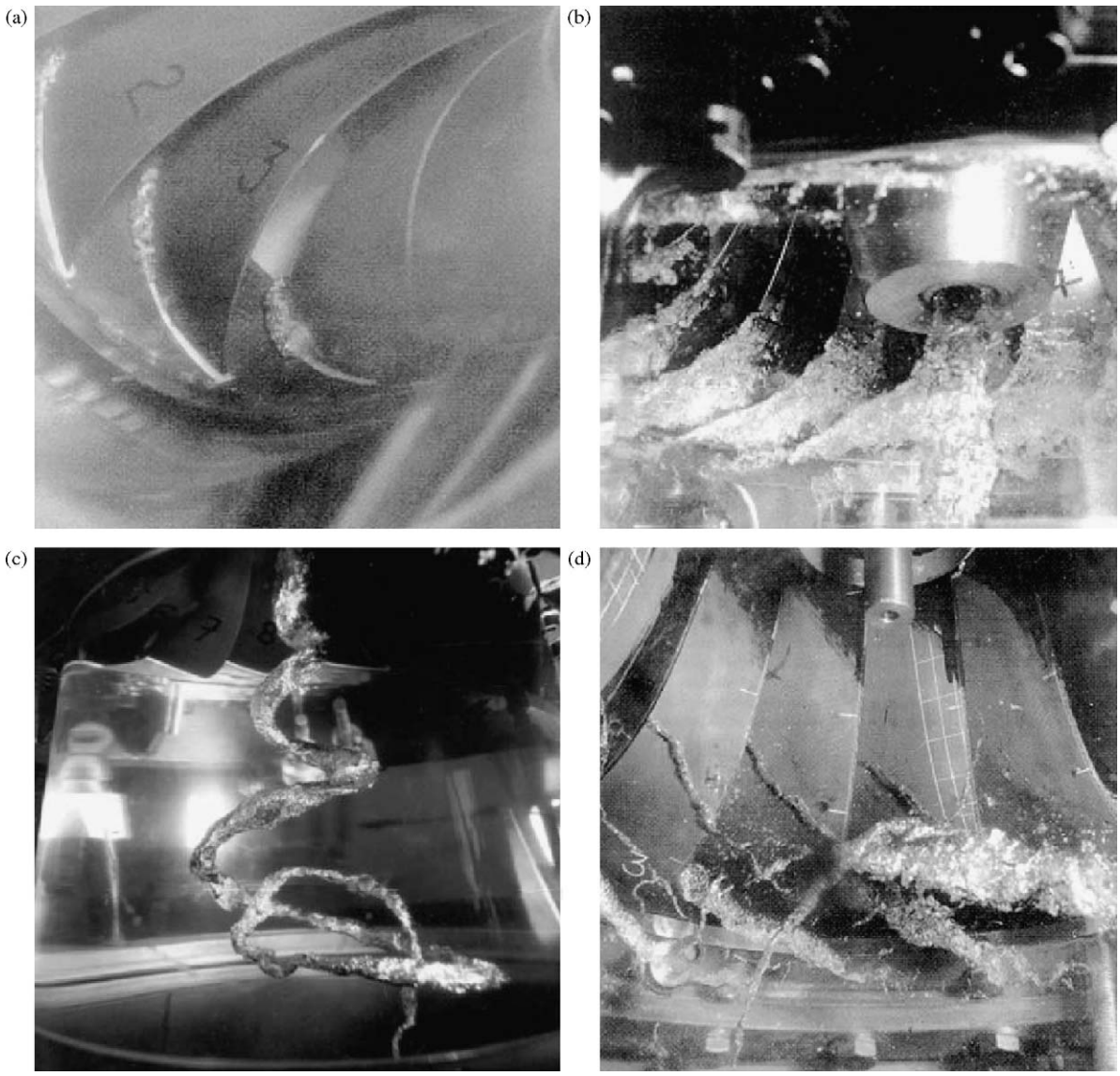

Fig. 3. Different types of cavitation in Francis turbines: (a) leading edge cavitation, (b) traveling bubble cavitation, (c) draft tube swirl and (d) interblade vortex cavitation.

where ρ is the density, V is the velocity vector, Γ is the effective exchange coefficient, and R_e and R_c are the vapor generation and condensation rate terms.

Nicolet et al. [18] carried out an investigation on scale model of high specific speed Francis turbines. The analysis of the resulting pressure fluctuation in the entire test rig shows significant pressure amplitude mainly at 2.46 fn, which evidences the excitation mechanism. A component of pressure fluctuation at ~2.5 fn frequency was identified all along the draft tube walls, the source of those pressure fluctuations being located at the inner

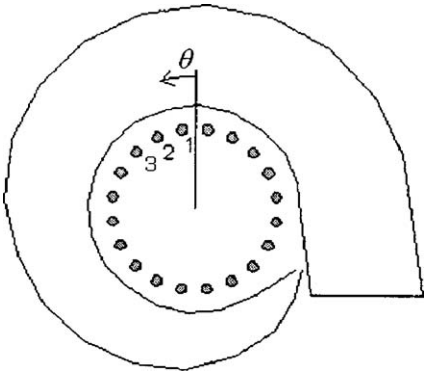

Fig. 4. The sensors placed on the 20 guide vanes react cavitation in various locations around the spiral.

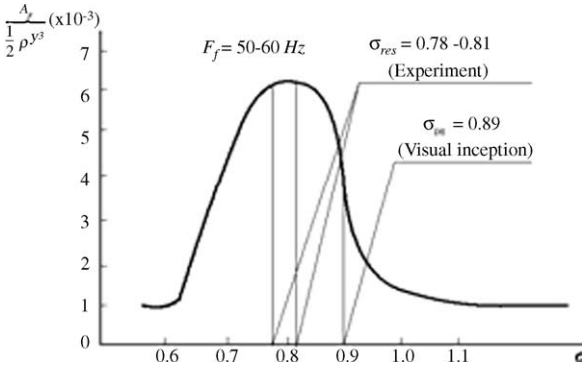

Fig. 5. Cavitation resonance from the UM Venturi.

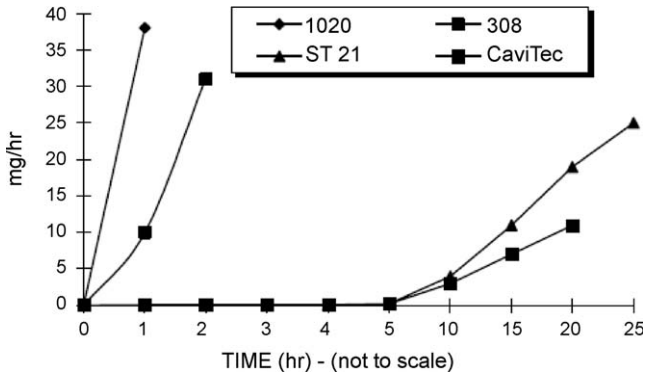

Fig. 6. Cumulative weight loss of various industrial alloys.

part of the draft tube elbow. The analysis of the pressure fluctuations phases for the ~2.5 fn frequency provides a way to determine the experimental wave speeds along the draft tube, which were the key parameters for a numerical simulation of the hydro-acoustic behavior of the test rig. The simulation carried out for the full test rig, taking into account piping, circulating pumps and the scale turbine model with the elbow draft tube showed that the ~2.5 fn frequency value corresponds to an eigen frequency of the system.

Hart and Whale [19] carried out work on improved weld surfacing alloy which was developed and tested to resist cavitation–erosion in hydro turbines. Typical wear characteristics experienced in laboratory testing correlated to actual service conditions. A metallurgical evaluation showed that a high strain, work hardening austenitic stainless steel produces superior resistance to cavitational erosion. Several industrial alloys were evaluated using the vibratory and high velocity cavitation test, to produce a new alloy development in weld surfacing. Field testing showed an improvement in cavitation–erosion resistance of up to 800% relative to 308 stainless steel. The cumulative weight loss of various industrial alloys are shown in Fig. 6.

Jean-Francois et al. [20] presented a comprehensive research effort aimed at understanding the influence of flow unsteadiness on leading edge cavitation. Pressure measurements were made on the suction side of an oscillating hydrofoil in the high speed cavitation tunnel. Leading edge roughness effects were investigated for both cases of fixed and oscillating hydrofoils. The cavity that detaches on the rough leading edge was thicker while its length was approximately the same as for the smooth configuration. Pressure fluctuations in the cavity closure region were higher for the rough configuration. It was observed that the cavity detaching on the smooth leading edge at fixed incidence can be completely vanish when the hydrofoil oscillates (Fig. 7).

The term cavitation was used to describe the phenomenon of liquid-to-gas and gas-to-liquid phase changes that occur when the local fluid dynamic pressures in areas of accelerated flow drop

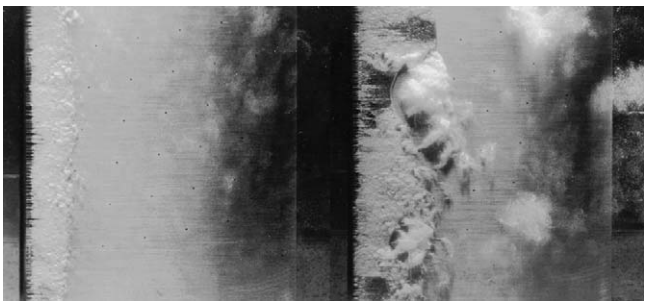

Fig. 7. Stable (left) and unstable (right) leading edge cavities.

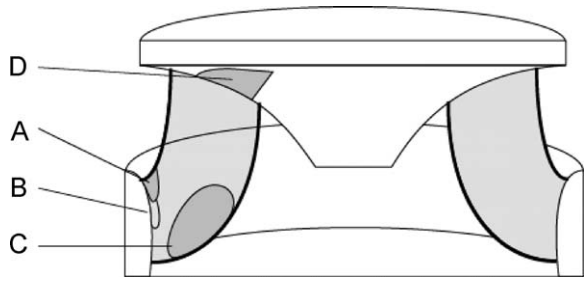

Fig. 8. Typical eroded areas of a Francis runner.

below the vapor pressure of the local fluid [21]. The liquid-to-gas phase change was akin to the boiling of water, except that it occurred at ambient temperatures. The gas-to-liquid phase change produced extremely high local pressures as vapor cavities implode on themselves. Cavitation commonly occurred in hydroelectric turbines, generally appearing around guide vanes, wicket gates, the turbine runner, and in the draft tube. Usually, cavitation within the fluid stream is not damaging to the turbine. However, when implosions occur near solid boundaries within the machine, flow surfaces can be damaged and eroded. Detection of the cavitation phenomenon is straight forward. Large increases in noise, particularly in moderately high frequency ranges (15–100 kHz) are characteristic of cavitation. In addition, vibration levels generally increase. However, in a machine condition monitoring program, the simple ability to detect cavitation is not too beneficial. The real need is to learn when the cavitation is damaging parts of the machine.

Avellan [22] found out that design, operation and refurbishment of hydraulic turbines, pumps or pump–turbine were strongly related to cavitation flow phenomena, which may occur in either the rotating runner–impeller or the stationary parts of the machine. The study presented the cavitation phenomena featured by fluid machinery including type of cavity development related to the specific speed of machines in both pump and turbine mode, the influence of the operating conditions, such as load, head and submergence. Therefore, for each type of cavitation illustrated by flow visualization made at the EPFL testing facilities, the influence of cavitation development on machine efficiency, operation and integrity were also discussed in Figs. 8–14.

Grekula and Bark [23] carried out an experimental study on cavitation processes in a Kaplan model turbine and studied with the aim to identify mechanisms that promote erosive cavitation. The studies were carried out with high-speed filming, video filming and visual observations with stroboscopic light. A periodic pattern of the cavitating tip vortex was observed. Cavitation at blade root observed as shown in Fig. 15. The main feature of the pattern was that the cavitating vortex was bent towards the blade surface and transformed into cloud formations. It was also found that these

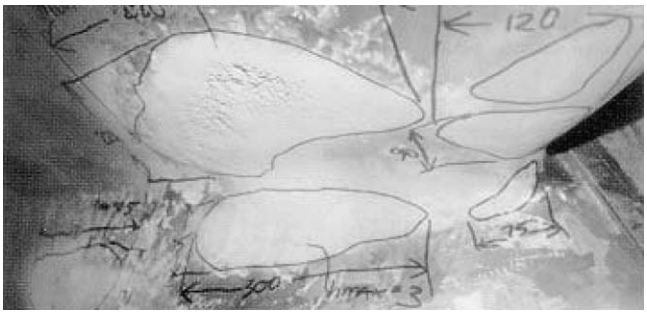

Fig. 9. Typical erosion at the wall of the blade suction side due to inlet edge cavitation, shaded area A of Fig. 8.

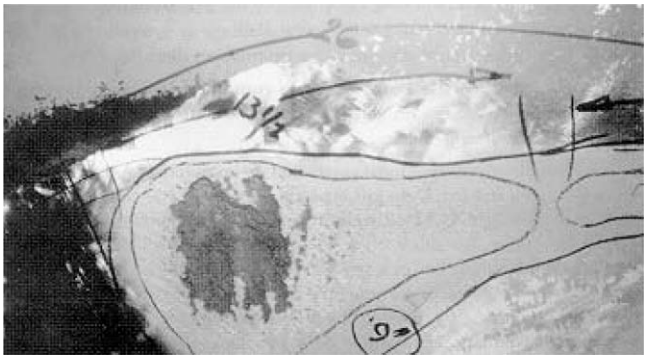

Fig. 10. Typical erosion at the wall of the blade suction side due to inlet edge cavitation, shaded area B of Fig. 8.

Fig. 12. Typical erosion at the wall of the runner hub due to interblades cavitation vortices, shaded area D of Fig. 8.

cloud formations appears in bands, with a periodicity which corresponds approximately to the spacing of the guide vanes. Moreover, the tip vortex cavitation was characterized by fine-scaled cloud cavitation at the points where it approached the blade surface, which indicated an erosion risk.

Harano et al. [24] investigated two splitter-blade-fitted runners installed in the Francis turbines. The splitter-blade-fitted runner was a practical application achieved through joint research, utilizing the latest fluid-analysis technology, model testing, strength analysis, etc., between Hitachi and The Kansai Electric Power Co., Inc. The relationship between inlet diameter and outlet diameter of Francis turbine is shown in Fig. 16. Results on vibration between turbine metal case and draft tube are shown in Fig. 17.

Szkodo [25] carried out an experimental investigation of cavitation resistance of Fe–Cr–Mn coating. The alloy was used in mending of machine elements subjected to cavitation. Chromium nickel stainless steel 0H18N9 was used as the substrate. The investigated sample was exposed to cavitation loading at the rotating disk facility. The investigations were performed in the initial period of the clad damage. The plastic deformation on the investigated surfaces was defined using an image analysis. The microstructure, chemical composition and phase identification of the modified layer were examined using scanning electron microscopy (SEM), light microscopy (LM), energy dispersive X-ray spectroscopy (EDX) and X-ray diffractometry (XRD), respectively. The hardness of processed layers was investigated by a Vicker hardness tester. The results indicated that there was different susceptible to plastic deformation caused by cavitation loading for different kind of laser processing (Fig. 18).

Nicolet et al. [26] investigated is a 1 GW, four Francis turbines power plant. Francis turbines feature a cavitating vortex rope in the draft tube resulting from the swirling flow of the runner outlet. For hydraulic system modeling hyperbolic differential equations are

$$\frac{\partial h}{\partial t}+\frac{a^2}{gA}\frac{\partial Q}{\partial x}=0 \tag{10}$$

$$\frac{\partial h}{\partial x}+\frac{1}{gA}\frac{\partial Q}{\partial t}+\frac{\lambda|Q|}{2gDA^2}Q=0 \tag{11}$$

where 'a' is the wave speed (m/s), 'Q' is the discharge (m^3/s), 'h' is the piezometric head (m), 'D' is the pipe diameter (m), 'A' is the cross-section (m^2), 'g' is the gravity (m/s^2) and 'λ' is the friction loss coefficient. The unsteady pressure field related to the precession of the vortex rope induces plane wave propagating in the entire hydraulic system. The simulation results revealed the piping natural frequencies that were excited by the draft tube pressure source. In addition, the transfer function between the draft tube pressure source and the generator electromagnetic torque pointed out the risk of electrical power swing. However, the risk can be really evaluated only knowing the pressure excitations and the draft tube wave speed. If the first one can be obtained from scaled model testing, the latter has to be estimated, either experimentally from vortex rope photography, or in the future, by CFD. The methodology was a helpful tool for predicting the risks of

Fig. 11. "Frosted" area at the wall of the runner blade trailing edge due to outlet traveling bubble cavitation, shaded area C of Fig. 8.

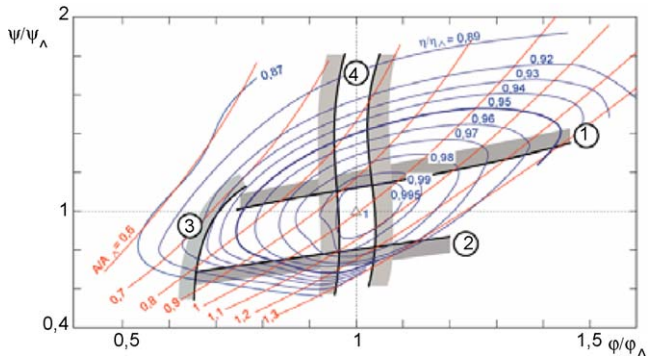

Fig. 13. Limits of cavitation development within the operating range of a Francis turbine. (1) Suction side leading edge cavitation limit; (2) pressure side leading edge cavitation limit; (3) interblade cavitation vortices limit; (4) discharge ring swirl cavitation limits.

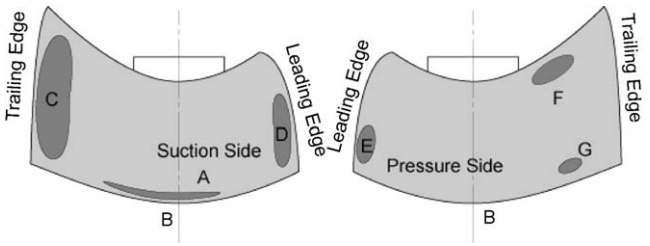

Fig. 14. Typical eroded areas of a Kaplan runner.

resonance at the early stages of pre-design or as a help for on site diagnostic purposes.

4. Analytical investigations

Muntean et al. [27] carried out a numerical investigation of the cavitating flow in a Francis turbine runner. First, the steady non-cavitating relative flow was computed in a runner interblade channel using the mixing interface approach. Second, the cavitation model was activated. Results for cavity shape and extent, as well as for the pressure distribution on the blade with and without cavity were presented and discussed. The equation of pressure coefficient (C_p) was as given below:

$$C_p = \frac{p - p_{ref}}{\rho E_{ref}} \tag{12}$$

where p_{ref} is the reference pressure, ρ is the density and E is the specific energy.

Qian et al. [28] carried out a three-dimensional unsteady multiphase flow simulation in the whole passage of Francis hydraulic turbine. The pressure pulsation was predicted and compared with experimental data at different positions in the draft tube, in front of runner, guide vanes and at the inlet of the spiral case. The relationship between pressure pulsation in the whole passage and air admission was analyzed. The computational results showed that air admission from spindle hole decreased the pressure difference in the horizontal section of draft tube, which in turn decreased the amplitude of low-frequency pressure pulsation in the draft tube; the rotor–stator interaction between the air inlet and the runner increases the blade-frequency pressure pulsation in front of the runner.

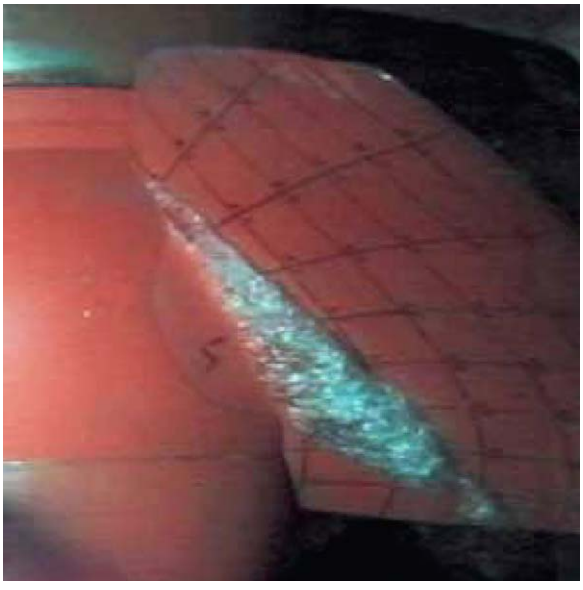

Fig. 15. Cavitation at the blade root.

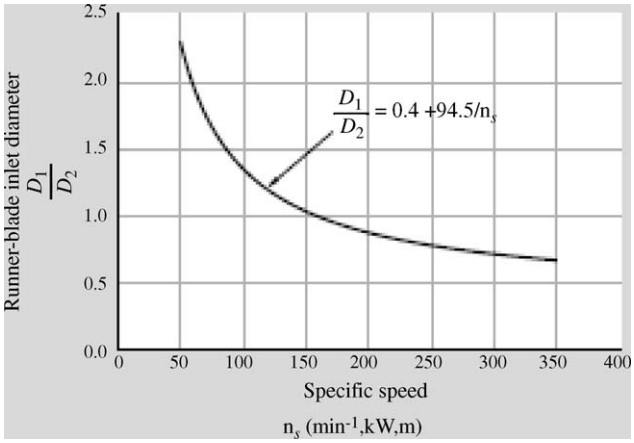

Fig. 16. Relationship between inlet and outlet diameter of Francis turbine.

Bajic [29] worked out novel technique for vibro-acoustical diagnostics of turbine cavitation and its use demonstrated on a Francis turbine. The technique enabled identification of different cavitation mechanisms functioning in a turbine and delivered detailed turbine cavitation characteristics, for each of the mechanisms or for the total cavitation. The characteristics specified the contribution of every critical turbine part to the cavitation intensity. Typical diagnostic results were obtained as enabled optimization of turbine operation with respect to cavitation erosion, showed it how a turbine's cavitation behavior can be improved; and formed the basis for setting up a high-sensitivity, reliable cavitation monitoring system.

Yuliun et al. [30] carried out a study of cavitating flow in a Kaplan turbine having numerical simulation with a cavitation model and a mixture two-phase flow model, which are in commercial code Fluent 6.1. It was performed to unsteady cavitating turbulent flow within the entire flow passage of a Kaplan turbine in a hydraulic power plant. Based on the calculation results, region and degree of cavitation occurred in the flow passage of the turbine running in a given working conditions.

Muntean et al. [31] carried out numerical investigation of the 3D flow in the distributor (stay vanes and guide vanes) of the GAMM Francis turbine. The domain corresponded to the distributor (stay vane and guide vane) interblade channel. There were

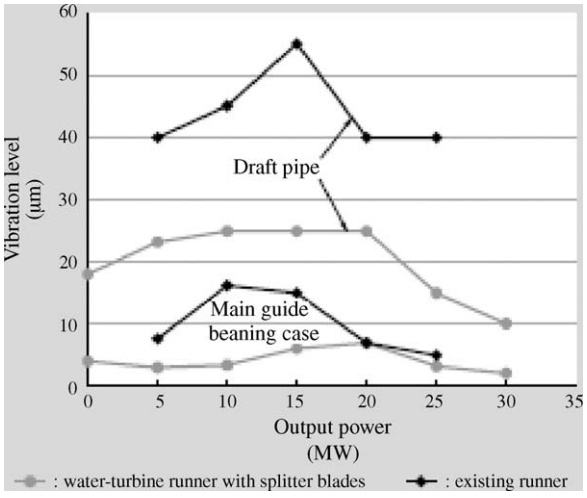

Fig. 17. Results on vibration between turbine metal case and draft tube.

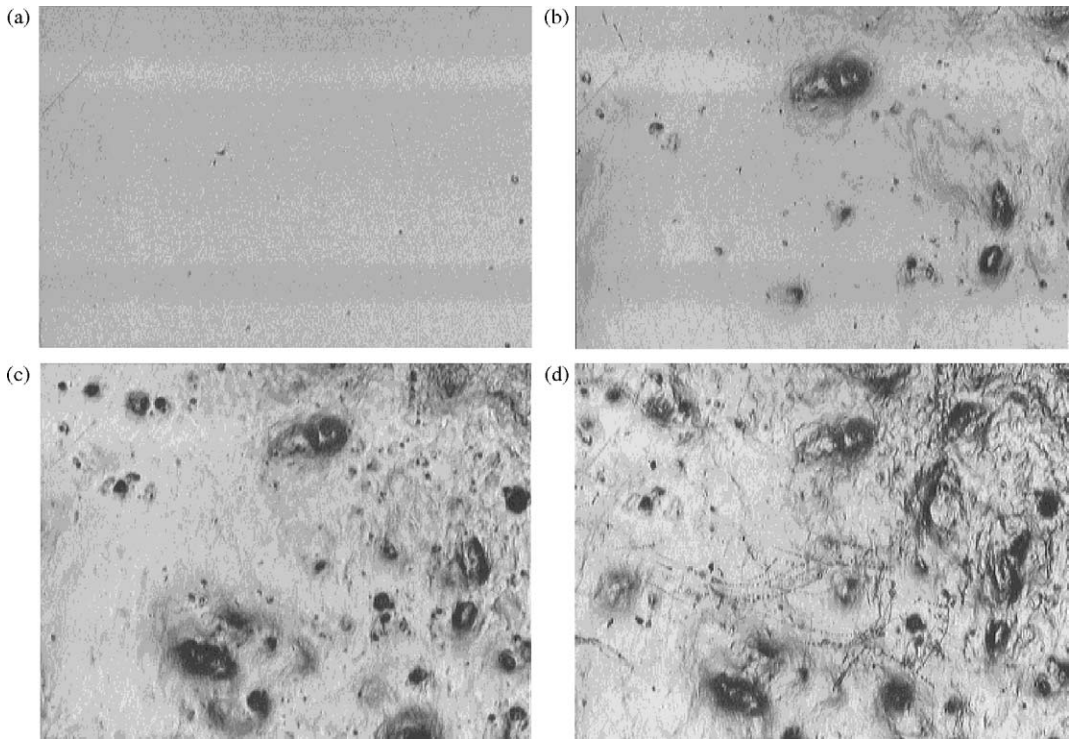

Fig. 18. Sample surface after grinding and polishing—(a) after 2 min, (b) after 4 min, (c) after 5 min and (d) after 7 min of cavitation erosion.

three main issues addressed in the paper: first, using the numerical methodology presented above, the distributor flow for several guide vane angle values was computed as shown in Fig. 19. As a result, the guide vane torque versus guide vane opening angle was computed for the actual position of the guide vane axis; second, it was investigated the flow for the whole range of the guide vane positions, at four different locations of the guide vane axis. The optimization criterion considered was the minimization of the mechanical loading of the turbine regulating system. This means that the extreme value of the torque applied to the guide vane shaft has to be minimized. The designed parameter to be optimized is the location of the guide vane shaft axis along the guide vane chord line.

Nilsson and Davidson [32] a parallel multiblock finite volume CFD code CALC-PMB (parallel multiblock) for computations of turbulent flow in complex domains was developed for an

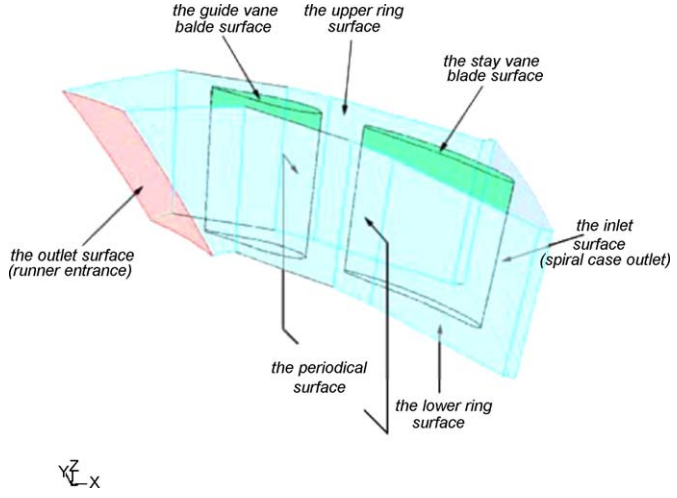

Fig. 19. Three-dimensional computational domain for the GAMM Francis turbine distributor.

investigation of the turbulent flow in Kaplan water turbines. This work was focused on tip clearance losses, which reduced the efficiency of a Kaplan water turbine by about 0.5%. The computational results from four different operating conditions, with different guide vane angles, were compared in the work. It was found that, the computations capture a vortical structure close to the leading edge tip clearance, where the tip clearance flow interacts with the shroud boundary layer and cavitational bubbles are formed. The tip blade loading increased when the specific speed decreased. Detailed measurements need to be performed, for use as boundary conditions and validation of the results.

Gagnon and Deschenes [33] focused on unsteady rotor–stator interaction in a propeller axial turbine. The flow behavior was analyzed at different rotor and stator relative locations with numerical simulations using a commercial code and k–e turbulence model. The main goal was to study unsteady flow phenomena such as wake, separation, forces and pressure fluctuations in the propeller turbine. This investigation will help to design a series of flow measurements used in turn to improve future CFD simulations with realistic velocity profiles as boundary conditions. Wakes and unsteady rotor–stator interactions for a different operating regime of a propeller turbine was studied. The wake behind guide vanes was dissipating very fast. It was not predicted whether it had an effect on the rotor stator unsteady interactions since higher harmonics of the spectrum were not well defined. The main interaction was therefore attributed to the pressure field fluctuations. Finally, the upcoming experimental phase to increase our knowledge and understanding of the propeller turbine flow may be looked forward.

Susan-Resiga et al. [34] carried out a numerical analysis of the swirling flow downstream through a Francis turbine runner. It was found that the flow stability characteristics were changed when decreasing the discharge. In Fig. 20 it was shown that the swirling flow in the survey section downstream the runner, in the draft tube cone, reached a critical state in the neighborhood of the best efficiency operating point. For larger discharge, the swirling flow

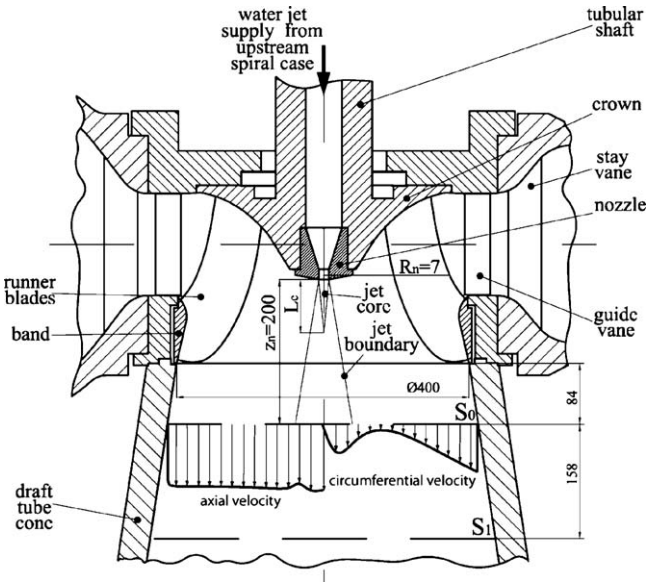

Fig. 20. Jet control technique for swirling flow in the discharge cone of Francis turbines.

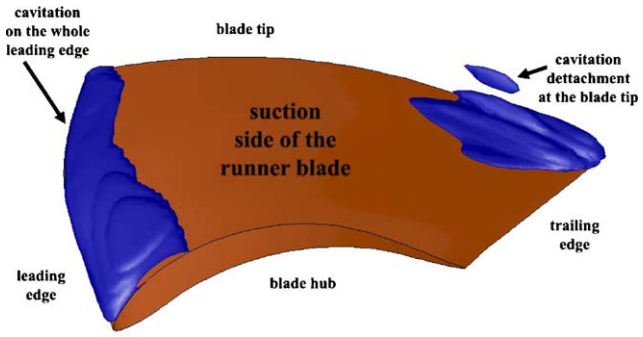

Fig. 22. Cavitation details in the runner domain in high cavitating operation.

was supercritical, and thus it was not able to sustain ax symmetrical perturbations. However, at partial discharge the flow became subcritical and it was able to sustain ax symmetric perturbations. Further investigations revealed that the axial velocity and specific energy deficit in the central region were responsible for the helical vortex breakdown, also known as "precessing vortex rope".

Aschenbrenner et al. [35] used the mixture model and full cavitation model to compute the unsteady turbulent flow and compared with experiment. From the vaporization and condensation mechanics between vapor and liquid and the assumption of unchanged pressure in cavity, the mass change rate of cavity was proportional to liquid pressure and vapor pressure difference.

Nennemann et al. [36] studied blade surface and discharge ring cavitation with an emphasis on the latter using CFD. Localized high flow gradients (cavitation) as well as more global unsteady effects (rotor stator interaction) contributed to the phenomena requiring advanced and resource intensive CFD approaches, notably locally refined meshes coupled with unsteady computations including runner rotation. CFD results enabled to explain the presence of discharge ring cavitation at distinct circumferential locations corresponding to the number of guide vanes used unsteady pressure measurements and high-speed camera images to qualitatively support the validity of our CFD model. Ultimately it was found that the CFD results enabled to understand the physics underlying the problem of discharge ring cavitation. Extensive parameters were studied to investigate all the significant influence factors as shown in Fig. 21.

Balint [37] carried out a numerical investigation by computing the 3D turbulent single phase flow in the Kaplan turbine runner, the secondary phase for the water (vapor) was activated starting far from the cavitation occurrence conditions. The output pressure in the runner domain was decreased to initiate the cavitating conditions on the runner blades. The unsteady solver with reduced time step size was employed to capture the self-induced cavitation in the runner domain and 3D effects together with wall-friction modification onto the runner blades. The shock of the unsteady cavitating flow leads to high distortion of the flow ingested downstream by the draft tube of the turbine. It was concluded that unsteady effects of the flow have been made mainly by the unsteady detachments of the cavitation at the blade suction side close to the trailing edge. An original method of computing the cavitation inception and of comparing different operating regimes in similar cavitating conditions was presented by plotting the cavitation volume growth as shown in Fig. 22.

5. Case studies

Bauer et al. [38] explored the techniques for the purpose of visualizing isolated flow structures in time-dependent data. Primary industrial application was the visualization of the vortex

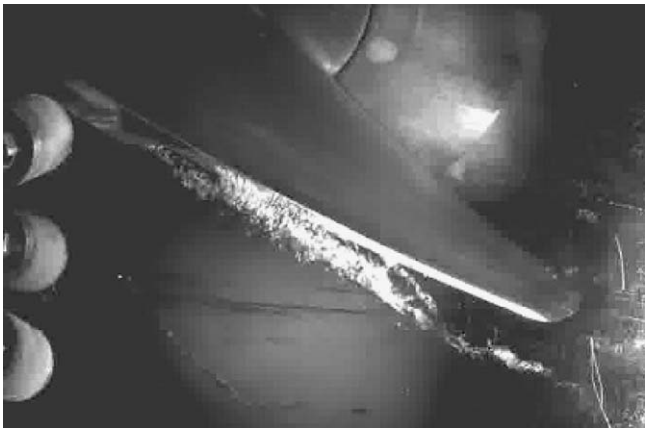

Fig. 21. Tip gap and tip gap vortex cavitation on a model Kaplan runner.

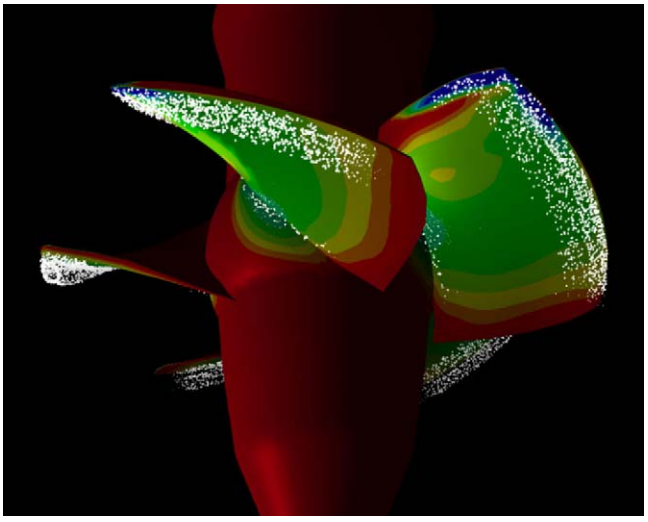

Fig. 23. Cavitation bubbles near Kaplan runner blades.

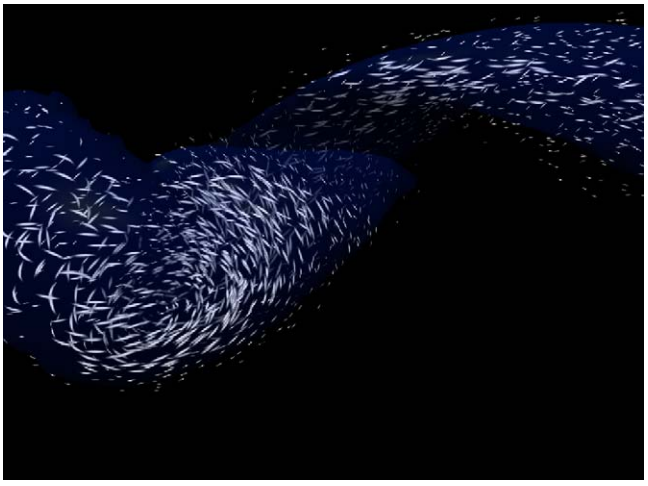

Fig. 24. Vortex rope in Francis draft tube.

rope, a rotating helical structure which builds up in the draft tube of a water turbine. The vortex rope can be characterized by high values of normalized helicity, which is a scalar field derived from the given CFD velocity data. In two related applications, the goal was to visualize the cavitation regions near the runner blades of a Kaplan turbine and a water pump as shown in Fig. 23. Again, the flow structure of interest can be defined by a scalar field, namely by low pressure values. A particle seeding scheme based on quasi-random numbers was proposed, which minimized visual artifacts such as clusters or patterns. By constraining the visualization to a region of interest, problems were reduced and storage efficiency was gained. They applied method to various data sets from our industry partners, visualizing the vortex rope in the draft tube of a Francis turbine shown in Fig. 24, and cavitation on the suction side of various turbine and pump runner blades. The concept of selectively visualizing relevant flow structures was proven to give additional insight into their complicated dynamic behavior.

6. Conclusions

Cavitation is a phenomenon of formation of vapor bubbles in low pressure regions and collapse in high pressure regions, high pressure is produced and metallic surfaces are subjected to high local stresses. It is difficult to avoid cavitation in hydro turbines which cannot be avoided completely, but can be reduced to an economically acceptable level. Many investigators have studied the process of cavitation in hydro turbines through experimental and analytical studies. Some of the investigators have reported that in spite of design changes in the turbine components and providing different materials and coatings to the turbine blades, however the improvement in most cases is not quite significant. It is therefore; further experimental and theoretical studies are required for studying the impact of cavitation in hydro turbine to determine impact of cavitation at different values of parameters which was relate to the cavitation in hydro turbine. CFD based analysis of cavitation in reaction turbines could be cost effective solution for an extensive analysis.

References

[1] www.powermin.nic.in-Ministry of power, Govt. of India.
[2] Tong D. Cavitation and wear on hydraulic machines. Int WP&DC)1981;(April).
[3] Lal J. Hydraulic machines, sixth edition, New Delhi: Metropolitan Book Co. Private Ltd.; 1975.
[4] Bansal RK. Fluid Mechanics and Hydraulic Machines; 1998. p. 839–41.
[5] Jain AK. Fluid Mechanics and Hydraulic Machines; 2002. p. 835–6.
[6] http://www.tev.ntnu.no/vk/publikasjoner/pdf/ArneKjolle/chapter14.pdfS.
[7] Duncan Jr W. Turbine manual. Facilities instructions, standards, & technique; 2000. p. 2–5.
[8] Farhat M, Bourdon P, Gagne J-L, Remillard L. Improving hydro turbine profitability by monitoring cavitation aggressiveness. In: CEA Electricity '99 conference and exposition; 1999.p. 1–15.
[9] Karimi A, Avellan F. Comparison of erosion mechanism in different types of cavitation. Wear 1986;113:305–22.
[10] Shi H, Li Z, Li Y. An online cavitation monitoring system for large Kaplan turbines. IEEE 2007;1–16.
[11] S. Alligné, Christophe N., Phillipe A., Basile K., Jean Jacques S., Francois A. Influence of the vortex rope location of a Francis turbine on the hydraulic system stability. IAHR 24th symposium on hydraulic machinery and systems, October 27–31. Foz Do Iguassu.
[12] Escalera X, Egusquiza E, Farhat M, Avellan F, Coussirat M. Detection of cavitation in hydraulic turbines. Mech Syst Signal Process 2008;20:983–1007.
[13] Bajic B. Methods for vibro-acoustic diagnostics of turbine cavitation. Hydro Dyn Res 2003;41:87–96.
[14] Li SC, Zuo ZG, Carpenter PW, Li S. Cavitation resonance. In: 5th int. symp. on cavitation; 2003.
[15] Wang W-Q, Zhang L-X, Yan Y. Large-eddy simulation of turbulent flow considering in flow wakes in Francis turbine blade passage. Hydrodyn Ser B 2007;19(2):201–9.
[16] Escaler X, Egusquiza E, Farhat M, Avellan F. Cavitation erosion prediction in hydro turbines from onboard vibrations. In: 2nd AHR symposium on hydraulic machinery and systems; 2004. B02-2.doc1 (10)-9.(10).
[17] Athavale MM, Li HY, Yu J, Singhal AK. Application of the full cavitation model to pumps and inducers. Rotating Mach 2002;8(1):45–56.
[18] Nicolet C, Jorge A, Francois A. Identification and modeling of pressure fluctuations of a Francis turbine scale model at part load operation. In: 22nd IAHR symposium on hydraulic machinery and systems; 2004.
[19] Hart D, Whale D. Review of cavitation–erosion resistant weld surfacing alloys for hydro turbines. www.castolin.com/wCastolin_com/pdf/publications/CaviTec.pdf.
[20] Jean-Francois C, Farhat M, Francois A. Physical investigation of the cavitation phenomenon. In: 6th international symposium on fluid control, measurement and visualization (Flucome 2000); 2000.
[21] Cavitation Detection in Hydraulic Turbines "Application to a Machine ConditionMonitoringSystem". www.usbr.gov/pmts/hydraulics_lab/hydstructures/cavitate.htm.
[22] Francois A. Introduction to cavitation in hydraulic machinery. In: The 6th international conference on hydraulic machinery and hydrodynamics; 2004.p. 11–22.
[23] Grekula M, Bark G. Experimental study of cavitation in a Kaplan model turbine. CAV2001:session B9.004.
[24] Harano M, Tani K, Nomoto S. Practical application of high-performance Francis–turbine runner fitted with splitter blades. Hitachi Rev 2006;55(3):109–13.
[25] Szkodo M. Effect of laser heating on cavitation behavior of Fe–Cr–Mn coating. Adv Mater Sci 2004;1(5).
[26] Nicolet C, Herou J-J, Greiveldinger B, Allenbach P, Simond J-J, Avellan F. Methodology for risk assessment of part load resonance in Francis turbine power plant.. In: IAHR int. meeting of WG on cavitation and dynamic problems in hydraulic machinery and systems; 2006.
[27] Muntean S, Bernad S, Resiga R, Anton L. 3D caviating flow in hydraulic Francis turbines. mh.mec.utt.ro/AccordFluid/docs/pdfs/Muntean03wnm2.pdf.
[28] Qian Z-D, Yang J-D, Huai W-X. Numerical simulation and analysis of pressure pulsation in hydraulic turbine with air admission. Hydrodyn Ser B 2007;19(4):467–72.
[29] Bajic B. Multidimensional diagnostics of turbine cavitation. Fluids Eng 2002;124(December):943–50.
[30] Wu Y, Liu S, Chen Q. Unsteady caviating turbulent flow simulation in a Kaplan turbine. In: 2nd IAHR international meeting of the work group on cavitation and dynamic problems in hydraulic machinery and systems; 2007.p. 35–40.
[31] Muntean S, Susan-Resiga RF, Bernad S, Ioan A. Analysis of the GAMM Francis turbine distributor 3D flow for the operating range and optimization of the guide vane axis location. In: The 6th international conference on hydraulic machinery and hydrodynamics; 2004.p. 131–6.
[32] Nilsson H, Davidson L. A numerical investigation of tip clearance flow in Kaplan water turbines. Hydropower into the next century—III; 1999.
[33] Gagnon J-M, Deschenes C. Numerical simulation with flow feature extraction of a propeller turbine unsteady rotor–stator interaction. Hydraulic Machinery Laboratory, Laval University, Canada, 2007.
[34] Susan-Resiga R, Muntean S, Hasmatuchi V, Bernard S. Development of a swirling flow control technique for Francis turbines operated at partial discharge. In: 3rd German–Romanian workshop on turbo machinery hydrodynamics; 2007.
[35] Aschenbrenner T, Otto A, Moser W. Classification of vortex and cavitation phenomena and assessment of CFD prediction capabilities. In: Proceedings of the 23rd IAHR symposium on hydraulic machinery and systems; 2006.
[36] Nennemann B, VU Thi C. Kaplan turbine blade and discharge ring cavitation prediction using unsteady CFD. In: 2nd IAHR international meeting of the workgroup on cavitation and dynamic problems in hydraulic machinery and systems; 2007.
[37] Balint D. High performance computing of self-induced unsteadiness for cavitating flows in hydraulic turbo machinery. Romania: University Politehnica of Timisoara, National Center for Engineering of Systems with Complex Fluids, 2004.
[38] Bauer D, Ronald P, Mie S, Mirjam S.In: A case study in selective visualization of unsteady 3D flow; 2002.